A Single Phase Induction Motor Voltage Controller with Improved Performance

JOSEPH D. LAW AND THOMAS A. LIPO, SENIOR MEMBER, IEEE

Abstract—**Induction motors inherently operate with nearly constant airgap flux and therefore almost constant iron losses. When the load does not require full flux, conventional voltage controllers utilize thyristors in series with the motor to reduce airgap flux by decreasing the applied voltage. Thereby, iron losses decrease and the overall efficiency increases. However, thyristor voltage controllers tend to introduce harmonics into the current waveform which not only reduces motor efficiency but also causes harmonic pollution of the power lines. An improved voltage controller and control strategy for efficiency improvement of single phase induction motors is presented. In particular, thyristor voltage control by dynamic switching of the winding configuration is presented. Laboratory data for a voltage controller, thus enhanced, demonstrates a significant decrease in input motor current distortion and increase in efficiency below one-quarter load.**

INTRODUCTION

INTEREST in energy conservation has resulted in the use of voltage-controlled ac motors to improve efficiency. Prompted by the work of Nola [1], [2], these control schemes utilize thyristors in the lines of single-phase and three-phase motors to reduce the iron losses for loads which do not require full-rated flux. However, thyristor voltage controllers tend to introduce harmonics into the current waveform which not only reduce motor efficiency but also cause harmonic pollution in the power lines. This paper is concerned with an improved voltage controller and control strategy which substantially improves the current waveform below one-quarter load. The paper compares the performance of the proposed controller with a conventional power-factor controller and with motor operation at full voltage without a controller. Circuit details of the thyristor phaseback voltage controller used in obtaining the laboratory data is given. Duty cycle curves are presented for the tested machine.

PHASEBACK VOLTAGE CONTROL

The principles of phaseback voltage control can be understood by reference to Fig. 1 which shows a schematic diagram of a conventional single phase induction motor phaseback voltage controller. In this circuit, a triac or, alternatively, two inverse parallel connected SCR's are placed in series with the motor supply. Voltage control is implemented by varying the conducting time of the triac. Typical voltage and current waveforms observed during operation of the controller are illustrated in Fig. 2. The angle γ that expresses the period in electrical degrees, during which time the current is zero, is called the *hold-off angle*. The angle corresponding to the instant at which the triac is triggered on with respect to the voltage zero crossing is called the *firing delay angle*, α. Finally, the angle φ, or *phase delay angle* corresponds to the time between a voltage zero crossing and the instant at which the current first reaches zero following that voltage zero crossing. The angle φ is somewhat erroneously also called the power factor angle which is only true in the case of sinusoidal steady-state.

Voltage control of an induction machine can be implemented by simply retarding the arrival of the gate pulses to the oncoming triac. This delay, in turn, serves to adjust

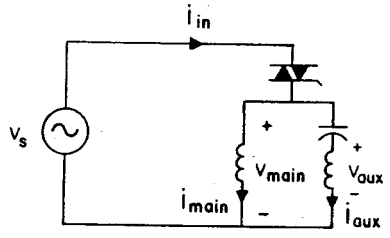

Fig. 1. Standard single-phase induction-motor voltage controller.

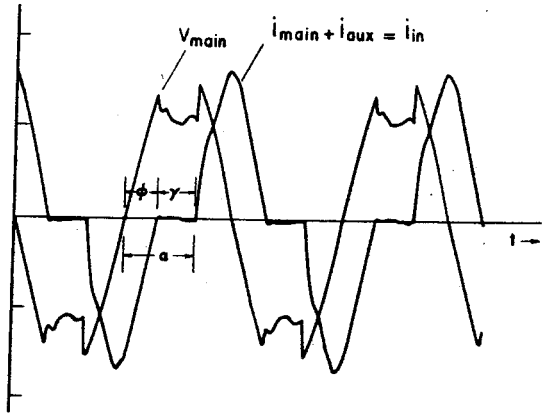

Fig. 2. Typical voltage and current waveforms and key control angles.

Manuscript received July 16, 1984; revised February 24, 1986. This paper was presented at the Power Electronics Specialists' Conference, Gaithersburg, MD, June 18-21, 1984.

J. D. Law was with the Department of Electrical and Computer Engineering, University of Wisconsin, Madison, WI. He is now with the Department of Electrical Engineering, Buchanan Engineering Laboratory, University of Idaho, Moscow, ID 83843.

T. A. Lipo is with the Department of Electrical and Computer Engineering, 1415 Johnson Drive, University of Wisconsin, Madison, WI 53706.

IEEE Log Number 8608644.

the hold-off angle γ. A nonzero angle γ results in a harmonic rich voltage waveform wherein the fundamental component across the load becomes less than the applied voltage. As a result, the air-gap flux of the motor is decreased and thus iron losses decrease correspondingly. To produce the same torque with the decreased air-gap flux, however, the slip must increase. The increase in slip gives rise to higher rotor copper losses. Whether stator copper losses increase or decrease depends upon the relative change of rotor currents with respect to magnetizing and iron loss currents. However, additional harmonic losses appear with phaseback control and tend to increase with an increase in γ.

It is of interest to note that there exists a value of voltage and corresponding hold-off angle for a particular load that will result in the highest motor efficiency. [3] makes a detailed analysis of the relative merits of several control variables that can be used to determine this hold-off angle. Nola correctly notes that this optimum value will remain constant for any load condition if all the machine parameters are constant [1]. However, changes in the motor parameters particularly due to saturation prevent such a simple interpretation. In particular, it has been found that a constant-phase delay-angle control scheme does not yield the optimal efficiency condition and control schemes of minimum input power, minimum delay angle, and minimum stator current yield results that are closer to the optimal [3].

In this paper the constant-phase angle control scheme of Nola is chosen as the control scheme to demonstrate the improvements possible by dynamically changing the winding configuration. Although not truly optimum, this type of control is familiar and easy to implement. While the concept of dynamically changing the winding configuration has not been explored for control schemes other than constant power-factor angle control, similar improvements are expected for other types of control algorithms.

Principle of Operation of New Thyristor Voltage Controller

The principle of operation of the improved single-phase induction motor controller can be understood by reference to Fig. 3. Fig. 3(a) shows, in schematic form, a specially wound single-phase permanent split-capacitor induction motor. The machine is wound with two identical circuits making up the main and auxiliary windings. Each main/auxiliary winding pair is connected in normal fashion with a permanent capacitor in series with each auxiliary winding. Under load conditions greater than one-quarter rated, triacs 2 and 3 are controlled and triac 1 is gated off. The circuit of Fig. 3(b) results. At rated load the full available supply voltage is applied to the machine windings so that the motor operates at full flux. When the load decreases, phaseback of the triacs result in a decrease in motor flux and an improved efficiency in the conventional manner. Upon reaching one-half voltage, corresponding to approximately one-quarter load, the hold-off angle γ of the

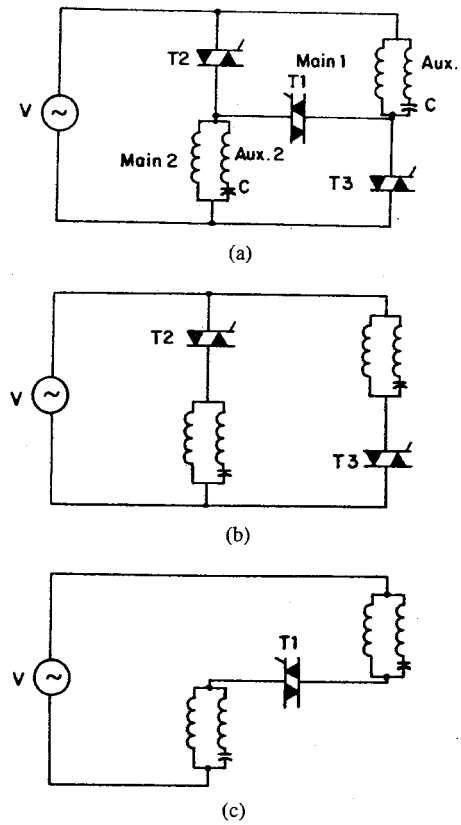

Fig. 3. Switching strategy of improved voltage controller. (a) Total circuit showing separation of main and auxiliary windings into two circuits. (b) Parallel connection for heavy loads. (c) Series connection for light loads.

triacs has increased to the point where motor winding currents and input current have a substantial harmonic content. However, if the windings are now dynamically switched such that triacs 2 and 3 are turned off and triac 1 is turned on, the circuit of Fig. 3(c) results. The half voltage condition across each circuit is preserved but can now be achieved with full conduction of the triac. Thus, the voltage waveforms across each motor circuit return to sinusoids. Losses in the motor clearly decrease accordingly. A substantial reduction of the rms input current can now be maintained over the parallel connection over the range from about one-quarter to zero load.

Implementation of a Thyristor Voltage Controller

A block diagram of the controller used to implement both the conventional and improved control strategies is shown in Fig. 4. A line voltage zero crossing detector is used to produce a signal, recognizable by the control logic, at the moment of each line voltage zero crossing. A current zero detector produces a signal, again recognizable by the control logic, indicating when the input current reaches zero. A control logic block determines the hold-off angle γ required to satisfy the phase delay angle command. An Intel 8748 microprocessor and 8 dual-in-line pin (DIP) switches constitute the hardware used to implement the control logic block. The 8 DIP switches

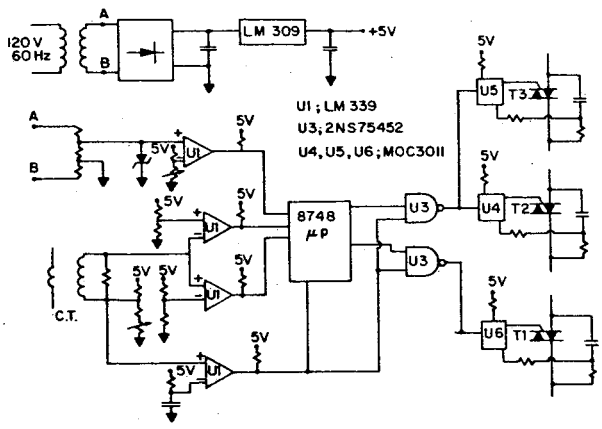

Fig. 4. Control logic and firing circuits for conventional and enhanced single phase voltage controller.

provide a means to input desired values for the phase-angle command φ^*.

To implement conventional power-factor control, only a single triac is needed and is placed in series with the applied voltage and motor windings. The motor windings are permanently fixed in a parallel circuit configuration. The control algorithm determines the delay angle φ by marking the instant of a voltage zero crossing and measuring the interval of time until the next current zero crossing. The dynamic operation of the control algorithm used in this paper can be understood by first considering the conventional single triac configuration. Assume initially that γ has been adjusted such that φ is equal to the command value φ^*. As the load on the controlled motor decreases, the motor appears as a more inductive load and φ becomes greater than φ^*. The controller responds by increasing γ, causing a decrease in the fundamental component of the applied voltage. This decrease in applied voltage results in a decrease in magnetization (reactive) current and air-gap flux. Rotor slip must increase to give rise to the greater rotor (predominantly real) current component needed to maintain the load torque. The overall effect is that the motor appears as a less reactive load than when the load first decreased. The controller continues to increase the hold-off angle γ until φ equals φ^*.

A similar but reverse motor effect and control response occurs for increases of the load up to a load corresponding to γ equal to zero. A hold-off angle equal to zero signifies that full supply voltage has been applied to the motor. The controller can now no longer maintain φ equal to φ^*, but simply sends gate pulses to the triac so as to allow full conduction.

The enhanced power-factor-controller three triac arrangement is configured in Fig. 3. The phase delay angle, φ, is determined in the same manner as in the conventional control algorithm. For loads greater than four-tenths rated load, the enhanced algorithm responds in exactly the same manner as the conventional controller. Referring to Fig. 3(b) the same parallel configuration is obtained by sending gating pulses to only triacs 2 and 3, leaving triac 1 off. For increases in φ or decreases in load, and γ at a value indicating that the load was at four-tenths load previous to the increase in φ, the algorithm responds by dynamically switching the winding configuration to series. Although a switchover of the winding configuration nearer to one-quarter load might be expected, the optimum value is influenced by the run capacitor values and resulting phase shift in the auxiliary windings. The four-tenths load point switchover was selected experimentally by evaluation of laboratory performance data. The dynamics of this change are explained in the next section.

Following the transition the motor windings are configured as shown in Fig. 3(c). Triacs 2 and 3 are held off and triac 1 conducts the motor current. The hold-off angle again equals zero. The control algorithm responds to further decreases in load by again increasing γ in the same fashion as for the parallel winding configuration.

When the load again begins to increase and becomes greater than four-tenths, the controller returns the windings to a parallel configuration. A hysteresis effect is provided to prevent chatter between the series and parallel configuration. This load point is identified by sensing that γ equals zero and φ is less than φ^* by a specified amount. The dynamics of this transition are also discussed in the next section.

Transitions Between Winding Configurations

Fig. 5 shows oscillograms of input current during a transition from series to parallel winding connections. Note that a small delay occurs after the current has gone to zero so as to decrease the chances of a line–line short. The transient currents that are present immediately following the transition decay within six cycles to a steady-state value. To supply the same torque with series windings, the motor must operate at a greater slip than with parallel windings. Thus, when the transition from series to parallel occurs, power input must increase momentarily to increase the speed slightly. Fig. 6 is an oscillogram of the instantaneous input power to the motor during the transition and shows the brief increase in power needed to reduce the slip.

Fig. 7 shows a scope trace of input current during the transition from a parallel to a series winding connection. In this case the motor runs at a larger slip for the same torque just before the transition. Since, in this case, the slip must increase, the triacs are programmed to remain turned off for three cycles so that the slip will inherently increase due to the motoring load. A less severe transient is apparent.

Performance Characteristics

Previous work on voltage controllers has shown that the phase delay angle for optimum performance is not necessarily the steady-state phase angle for rated torque [3]. In this case the optimum operating condition, for both series and parallel winding configurations, must be either analytically or, in this case, experimentally determined. A summary of the measured efficiencies obtained and the optimum values of φ^* is shown as a function of load

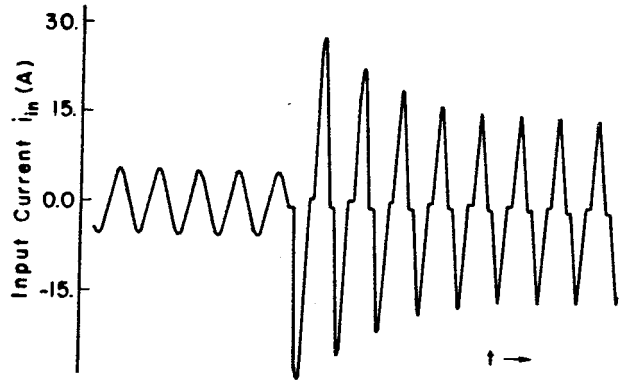

Fig. 5. Oscillograms of load current during transition from series to parallel connection.

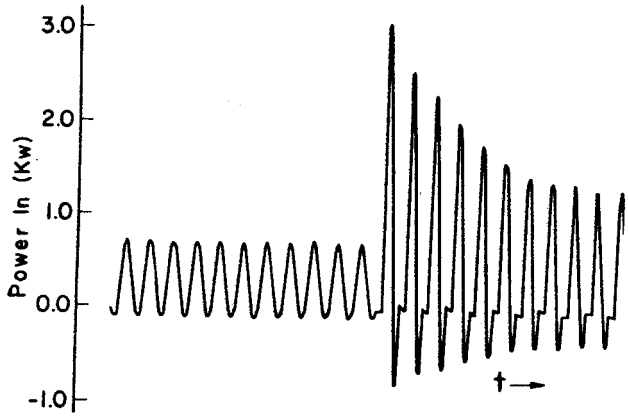

Fig. 6. Oscillogram of instantaneous power during transition from series to parallel connection.

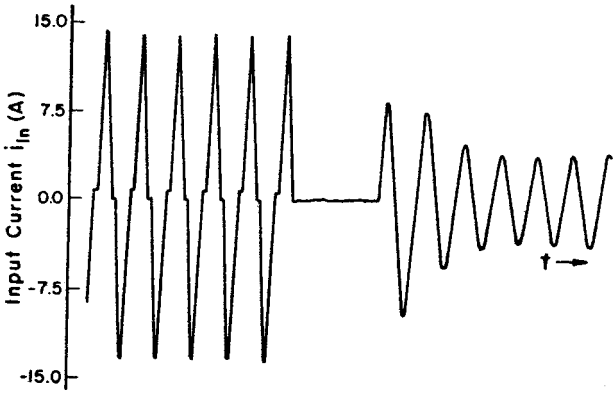

Fig. 7. Oscillogram of current transient during transition from parallel to series connection.

torque in Fig. 8. Figs. 9 and 10 give the corresponding fundamental component of voltage and slip used to obtain the curves of Fig. 8, respectively. To provide a basis for comparison, the performance curves obtained using both a constant voltage supply and an ideal constant slip controller with an adjustable sine-wave voltage supply are shown. The nameplate data and parameters for the motor used in the testing are recorded in the Appendix. In particular, the magnetizing reactance and core resistance of the main windings versus the air-gap voltage are provided

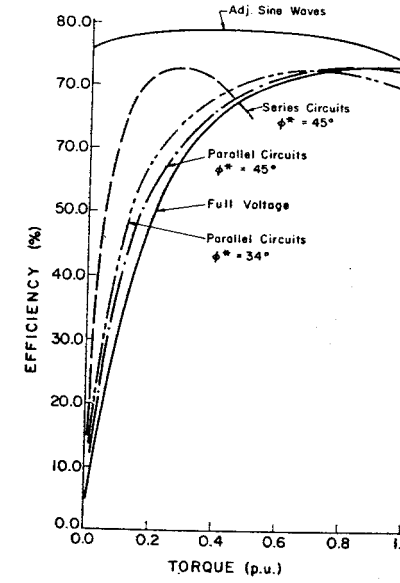

Fig. 8. Efficiency for series and parallel connection compared to full voltage operation and optimum adjustable sine waves.

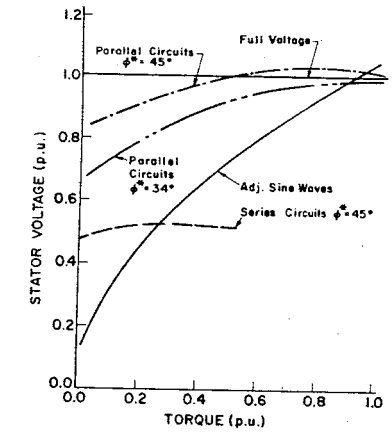

Fig. 9. Fundamental voltage component of voltage controllers corresponding to Fig. 8.

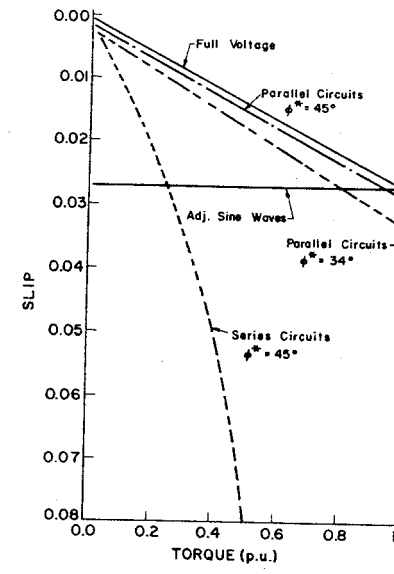

Fig. 10. Slip frequency of voltage controllers corresponding to Fig. 8.

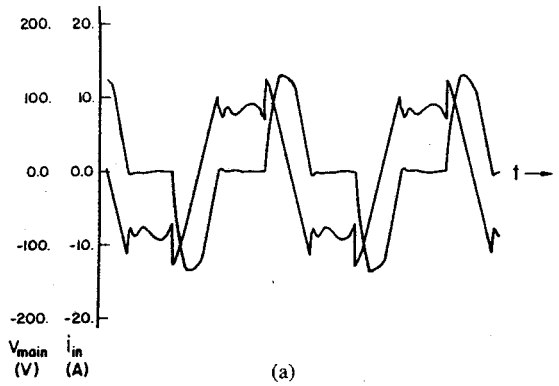

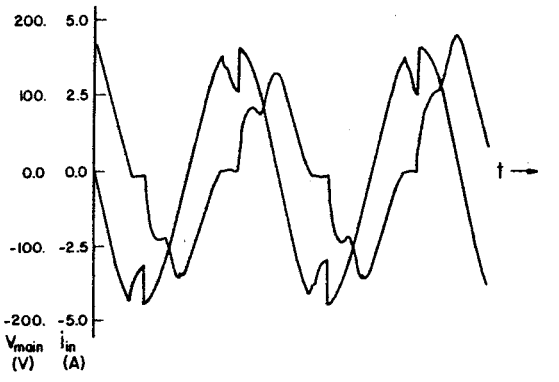

Fig. 12. Oscillogram of voltage and current. (a) Constant power factor controller with parallel windings. (b) Series windings for 0.02 per unit load torque.

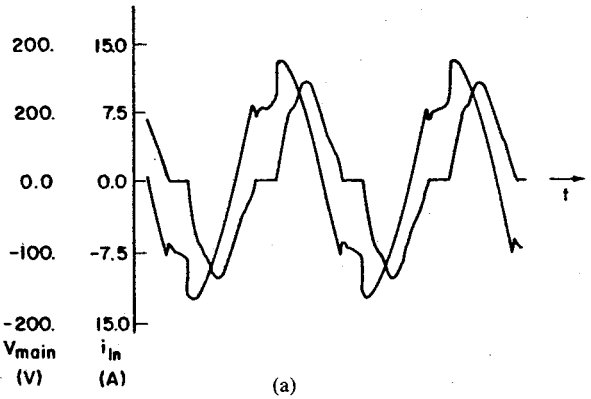

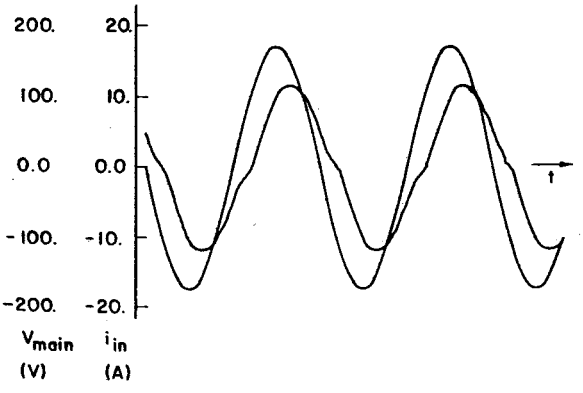

Fig. 13. Oscillogram of voltage and current. (a) Constant power factor controller parallel windings. (b) Series windings for 0.5 per unit load torque.

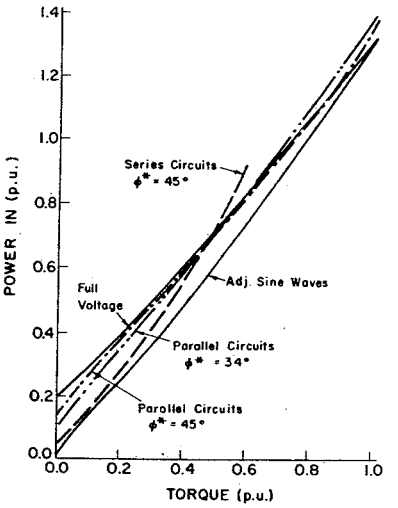

Fig. 14. Per unit power input versus per unit load torque for different control options.

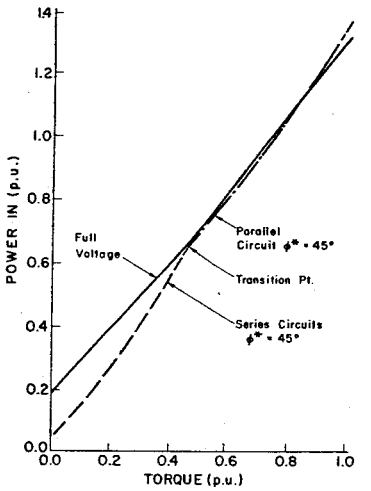

Fig. 15. Per unit power input versus per unit load torque for final modified controller.

phase control and with a parallel winding configuration only, the decrease in input power for low torques is counteracted by increases in input power for torques greater than one-half the rated load compared to a motor without phase control. Fig. 15 gives a comparison of power input for the enhanced controller and the motor without a controller. For torques below one-half, the input power saved with series windings and phaseback control is approximately twice that of parallel connections with φ^* equal to 34°. For torques above one-half pu a series winding connection results in a rapid increase in input power for increases in torque. However, at one-half torque the winding configuration is switched to parallel. The command delay angle of 45° with parallel windings continues to require less power input then an uncontrolled motor up to approximately eight-tenths load. For loads above this point the motor without a controller requires less power.

In [3] the concept of a duty cycle curve for a power-factor controller was introduced as a means for determin-

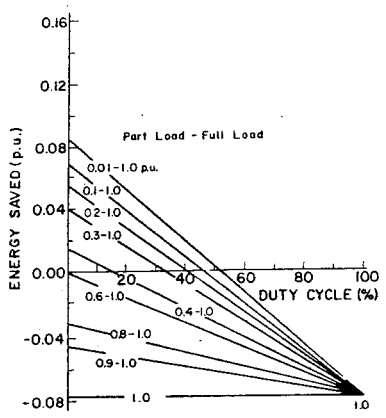

Fig. 16. Duty cycle curve for conventional power factor controller with $\varphi^* = 34°$.

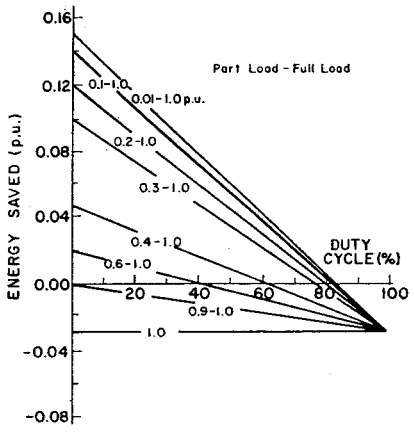

Fig. 17. Duty cycle curve for modified power factor controller with dynamic switching between parallel and series circuit, $\varphi^* = 45°$.

ing the energy savings possible in a given application. Such a curve is possible since in many motor applications a motor is subjected to two distinct load conditions. First, a heavy load condition occurs in which the motor is performing useful work. In this case, maximum efficiency is of primary concern. The second condition is basically an idling mode. For idle conditions the main goal is to minimize the input power.

Fig. 16 shows a duty cycle curve for the conventional controller using the motor described in Appendix A. The load is assumed to vary between one pu load and a fraction of rated load. The duty cycle is defined as the percentage of time spent at the full load condition. Hence, a duty cycle of 80 percent corresponds to a motor which operates 80 percent of the time at one per unit load and 20 percent at a fractional load. The value of the fractional load is the parameter of the straight line curves. Hence, the straight line corresponding to 0.4–1 indicates that the fractional load is 0.4 of rated load. Note that to reach a break-even point, a duty cycle of 54 percent or less is required even for part loads of 0.01 pu torque (i.e. no load). No savings are possible with the motor tested for part loads above six-tenths rated load.

A duty cycle for the enhanced controller is shown in Fig. 17. Savings are possible with the modified controller

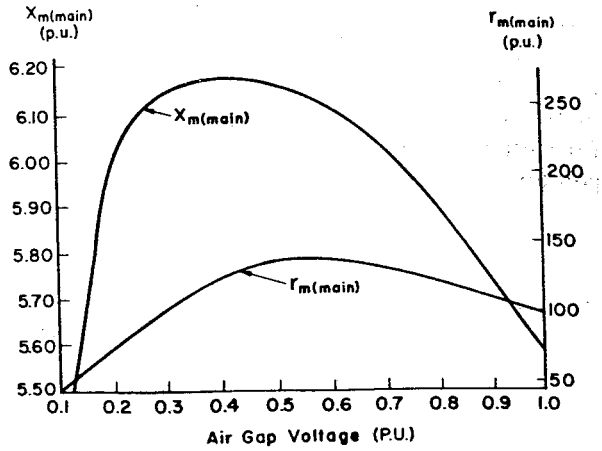

Fig. 18. Magnetizing reactance and core resistance of main winding of tested machine as a function of air-gap voltage.

for part loads below nine-tenths rated load. Also, savings are possible for duty cycles where the motor operates up to 83 percent of the time at 1.0 pu torque. The maximum savings is 14 percent of the motor input power which is a substantial improvement over the conventional voltage controller. Since Figs. 16 and 17 were constructed from actual measured data it is important to mention that these potential savings are real and not simply estimates.

While the transition from parallel to series circuits is accomplished at one-half voltage, this point can be modified, if desired, by suitable modification of the motor. For example, tapped windings could be used to move the transition point to any desired value. Also, variations of the modified voltage control strategy could be obtained by varying the ratio of circuit turns to values other than unity or by modifications in the triac location such that the triacs control voltage only across the main or the auxiliary windings. With the triacs connected only in series with the auxiliary windings, conduction losses could be reduced. Also, by varying γ the motor could be made to operate closer to a balanced two-phase condition than without a controller. If the triacs are placed only in the main winding, a single centrifugal switch or a solid-state switch could be used to make possible a capacitor start-capacitor run motor versus the two switches that would be required with the strategy presented in this paper.

Conclusion

An improved power-factor control scheme for a single-phase permanent split-capacitor induction motor accomplished by dynamically switching the winding configuration has been presented in this paper. Laboratory data shows a significant decrease in harmonic distortion of the input current and indicates a greatly improved efficiency for the modified voltage controller over the conventional voltage controller at reduced loads.

Acknowledgments

The authors are indebted to Raymond Timpone and the Marathon Electric Co. for donating the motor used for

this study. Dr. Chu Wang is thanked for his development of software which facilitated laboratory data acquisition. Finally the authors are grateful to the industrial sponsors of Wisconsin Electric Machines and Power Electronics Consortium (WEMPEC) for contributing financial support towards this project.

APPENDIX A
Nameplate Data

Marathon Electric Manufacturing Corporation

115/208-230 V	60 Hz
16/8 A	1725 r/min
1.5 hp	1.15 Service Factor

Per Unit Bases

$P_b = 1119$ W	$I_b = 9.73$ A
$V_b = 115$ V	$Z_b = 11.8\ \Omega$

Per Unit Parameters

Main Winding Stator Resistance:	$R_{sm} = 0.123$ pu
Auxiliary Winding Stator Resistance:	$R_{sa} = 0.572$ pu
Main Winding Rotor Resistance:	$R_{rm} = 0.186$ pu
Auxiliary Winding Rotor Resistance:	$R_{ra} = 0.457$ pu
Main Winding Leakage Inductance:	$X_{lm} = 0.271$ pu
Auxiliary Winding Leakage Inductance:	$X_{la} = 0.644$ pu
Main and Auxiliary Winding Magnetizing Inductance	See Fig. 18
Main and Auxiliary Winding Iron Loss Resistance	See Fig. 18

REFERENCES

[1] F. J. Nola, "Power factor control system for AC Induction Motor," U.S. Patent 4 052 648, Oct. 4, 1977.
[2] "Save power in AC induction motors," NASA technical brief no. MFS-23280, Summer 1977.
[3] T. M. Rowan and T. A. Lipo, "A quantitative analysis of induction motor performance improvement by SCR voltage control," *IEEE Trans. on Ind. Appl.*, vol. IA-19, pp. 545–553, July/August 1983.

Joseph D. Law was born in Madison, WI, on October 27, 1957. He received the B.S. degree from the University of Idaho, Moscow, in 1981 and the M.S. from the University of Wisconsin-Madison in 1985.

He worked for the Research Division of Carrier from 1984 to 1985. He is presently a member of the faculty at the University of Idaho.

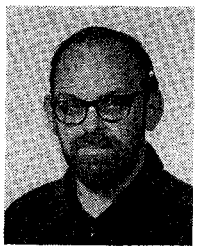

Thomas A. Lipo (M'64–SM'71) received the B.E.E. and M.S.E.E. degrees from Marquette University, Milwaukee, WI, in 1962 and 1964, respectively, and the Ph.D. degree in electrical engineering from the University of Wisconsin in 1968. He was an NRC postdoctoral fellow at the University of Manchester Institute of Science and Technology, Manchester, England, during 1968–1969.

From 1969 to 1979 he was an Electrical Engineer in the Power Electronics Laboratory of Corporate Research and Development of the General Electric Company, Schenectady, NY. While at General Electric, he helped pioneer the computer simulation of many types of converter systems including cycloconverters, pulsewidth modulation voltage inverters, current-source ASCI inverters, third harmonic commutated CSI inverters, and load commutated converters. He has also been heavily engaged in the development of algorithms for control of solid-state converter drives for which he has received several IEEE Prize Paper Awards including corecipient of the 1984 Best Paper Award for the IAS Transactions. He holds seven patents with one additional pending. He has published over 70 technical papers, contributing to the analysis and design of a wide range of industrial applications including ac drives for ball mills, pumped hydro, excavators, as well as traction drives for transit cars, locomotives, and off-highway vehicles. He is currently a Professor in the Department of Electrical and Computer Engineering, University of Wisconsin-Madison.

Dr. Lipo is Chairman of the IAS Industrial Drives Committee, an Ad Hoc Member of its Executive Committee, and serves on the IAS Fractional and Integral Horsepower Subcomittee. He also serves on the IES Drives Committee and the PES Synchronous Machine Subcomittee, Electric Machine Theory Subcommittee, and Induction Machine Subcommittee of which he is a past Chairman. He has also served on the Program Committee for the IEEE Power Electronics Specialists Conference for the past seven years and was Program Chairman in 1979. He is a member of the Steering Committee for the International Conference on Electrical Machines, an Associate Editor of the journal *Electric Machines and Power Systems*, and Editor of IEEE TRANSACTIONS ON POWER ELECTRONICS. He is a member of Pi Mu Epsilon, Eta Kappa Nu, Tau Beta Pi, and Sigma Xi.